IOP Conf. Series: Journal of Physics: Conf. Series **807** (2017) 032001 doi:10.1088/1742-6596/807/3/032001

Local moments in the heterogeneous electronic state of Cd-substituted $CeCoIn_5$: NQR relaxation rates

H. Sakai[1], F. Ronning[2], T. Hattori[1], Y. Tokunaga[1], S. Kambe[1], J.-X. Zhu[3], N. Wakeham[2], H. Yasuoka[2], E. D. Bauer[2], and J. D. Thompson[2]

[1] Advanced Science Research Center, Japan Atomic Energy Agency, Tokai, Ibaraki, 319-1195, JAPAN
[2] Condensed Matter and Magnet Science, Los Alamos National Laboratory, Los Alamos, New Mexico 87545, USA
[3] Theoretical Division, Los Alamos National Laboratory, Los Alamos, New Mexico 87545, USA

E-mail: sakai.hironori@jaea.go.jp

Abstract. We have used nuclear quadrupole resonance (NQR) to probe microscopically the response of a prototypical quantum critical metal $CeCoIn_5$ to substitutions of small amounts of Cd for In. Approximately half of the Cd substituents induce local Ce moments in their close proximity, as observed by site-dependent longitudinal nuclear spin relaxation rates $1/T_1$. To reaffirm that localized f moments are induced around the Cd substituents, we find a Gaussian spin-echo decay rate $1/T_{2G}$ of transverse nuclear spin relaxation. Further, T_1T/T_{2G}^2 for the NQR subpeak is found to be proportional to temperatures, again indicating local moments fluctuations around the Cd substituents, while that for the NQR main peak shows a $T^{0.7}$-dependence. The latter temperature dependence is close to 0.75 in pure $CeCoIn_5$ and indicates that the bulk electronic state is located close to a two dimensional quantum critical instability.

1. Introduction

Quantum critical points (QCPs) are an excellent organizing principle for the non-Fermi liquid (NFL) behavior observed in many systems and a source of fluctuations from which unconventional superconductivity (SC) emerges. $CeCoIn_5$ is an unconventional superconductor that belongs to the $CeTIn_5$ (T=Co, Rh, Ir) family, and is known to lie in close proximity to an AFM QCP at ambient pressure [1, 2]. A small amount of Cd ($5s^2$) substitution for In ($5s^25p$), induces long-range AFM order [3]. For $\sim$1% Cd substitution the AFM propagation vector is $\boldsymbol{Q} = (\frac{1}{2}, \frac{1}{2}, \frac{1}{2})$ and the ordered moment is $\sim$0.7 μ_B/Ce [4, 5]. Applying pressure suppresses the AFM; however, the fluctuations and the signatures in electrical transport properties at this pressure (P)-induced AFM QCP are absent [6]. The SC dome for $\sim$1% Cd substitution remains broad in the T-P plane as in the pure $CeCoIn_5$ [7]. Recently we reported a qualitative difference in local electronic environments around Sn and Cd substituents that were probed by nuclear quadrupole resonance (NQR). While Sn substitutions introduce a rather homogeneous electronic state suppressing the AFM fluctuations, Cd substitutions produce an electronic heterogeneous state where Cd substituents enhance AFM behavior by inducing unscreened localized moments in their immediate vicinity [8]. At the same time, the bulk electronic state far from the Cd substituents is the same as in the pure $CeCoIn_5$.

In this paper, the localized f nature in the vicinity of Cd substituents in $CeCoIn_5$ is further investigated by measuring the longitudinal and transverse nuclear spin relaxation rates.

2. Experimental

Single crystals of $CeCoIn_5$ and $CeCoIn_{4.925}Cd_{0.075}$ (1.5 % Cd-doped) were grown by the self-flux method [9]. Small crystals for zero-field NQR studies were selected from the same batch used for magnetic susceptibility, electrical resistivity and specific heat measurements. The AFM transition temperature T_N for the 1.5% Cd-doped sample is 3.7 K [8]. $CeCoIn_5$ forms in the tetragonal $HoCoGa_5$-type structure ($P4/mmm$) with two crystallographically inequivalent In sites denoted as In(1) ($4/mmm$) and In(2)($2mm$). Microprobe measurement using wavelength dispersive spectroscopy and extended x-ray absorption fine-structure (EXAFS) observe a homogeneous distribution of Cd with a preferential occupation on the In(1) site [10]. Consequently, the fractional occupancy for the substituted atoms on these In(1) and In(2) sites is roughly 50/50 [10]. NQR measurements were carried out using a phase-coherent, pulsed spectrometer. Using the conventional definition of the electric field gradient (EFG), the NQR frequency ν_Q is defined as $3e^2qQ/\{2I(2I-1)h\}$ by the nuclear quadrupolar moment eQ and the principal component of the EFG tensor $eq \equiv V_{ZZ}$. For a non-axial EFG, the asymmetry parameter is defined as $\eta \equiv \{|V_{YY}| - |V_{XX}|\}/|V_{ZZ}|$ ($|V_{XX}| \leq |V_{YY}| \leq |V_{ZZ}|$). The ^{115}In NQR spectrum for $CeCoIn_5$ consists of 4 lines for In(1) sites with an equal separation of ν_Q=8.17 MHz and η=0, and 4 unequally-separated lines for In(2) sites whose positions give ν_Q=15.5 MHz and η=0.39 [11], by diagonalization of the electric quadrupole Hamiltonian $\mathcal{H}_Q = (h\nu_Q/6)\{3I_z^2 - I(I+1) + (\eta/2)(I_+^2 + I_-^2)\}$.

The spin-echo inversion recovery method was used to determine the longitudinal nuclear spin relaxation rates $1/T_1$. The nuclear magnetization $M(t)$ was recorded as a function of time t after the inversion rf pulse, always together with recording $M(\infty)$ which is the echo intensity without an inversion pulse. The inversion pulse width was adopted to be $\sim$20 μsec as long as possible. To evaluate T_1, each $R(t)$ was fit by the recovery function for the $4\nu_Q$ transition line of $I = 9/2$ with a single T_1: $R(t) \propto (4/33)\exp(-3t/T_1) + (80/143)\exp(-10t/T_1) + (49/165)\exp(-21t/T_1) + (16/715)\exp(-36t/T_1))$, which is derived assuming an EFG $\eta = 0$. In the case of finite η, the recovery function was calculated by numerical diagonalization of the master equation for nuclear relaxation.[12] T_1 did not change significantly if a finite η of 0.01–0.1 was assumed in these cases.

The transverse nuclear spin relaxation rates $1/T_2$ were derived by fitting the echo decay $E(2\tau)$ to $E(2\tau) = E(0)\exp(-2\tau/T_{2L})\exp(-\frac{1}{2}(2\tau/T_{2G})^2)$ with τ being the separation time between excitation and refocusing pulses. In a strongly correlated metal, $1/T_2$ contains the T_1-process which is represented by Lorentz-type decay on a scale T_{2L} and an indirect (nuclear) spin-spin coupling by Gaussian-type decay with a time scale T_{2G}.

3. Results and Discussions

Figure 1 shows a summary of our findings in the 1.5% Cd-doped $CeCoIn_5$ reported in Ref. [8]. As seen in Fig. 1(a), the $4\nu_Q$ line for In(1) splits into a main peak (A) and two satellite peaks labeled B, and C. The split In(1) spectrum for the Cd case is consistent with previous reports [5]. The resolved line splitting means that the local EFGs for the A, B, and C peaks are discretely distributed for sites near Cd. We can estimate η for A, B, and C sites for Cd substitutions to be 0.005, 0.09, and 0.12, respectively. For spectral assignment, EFGs have been calculated by density functional theory (DFT) assuming 2.5% Cd-doping in a $2 \times 2 \times 2$ supercell [8]. These calculations reproduce the main NQR spectral features, e.g., the In(1) NQR lines are discrete. From a comparison with the calculations, B and C lines can be assigned to the nearest neighbor In(1) sites for Cd substituted on In(2) (hereafter, Cd(2) dopants) and In(1) (Cd(1) dopants) sites, respectively. The respective peak dependences of the longitudinal nuclear spin relaxation rates $1/T_1$ for the In(1) sites, as seen in Fig. 1(b), show a striking enhancement of $1/T_1$ just

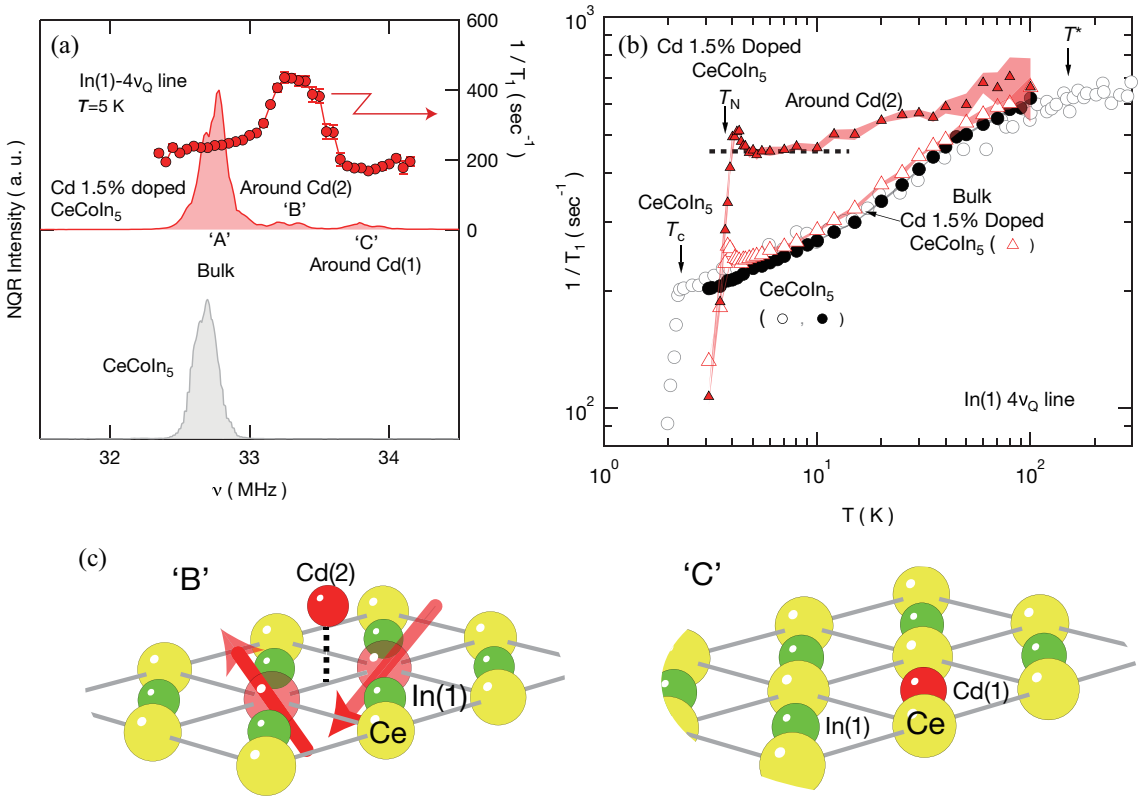

Figure 1. (a) ^{115}In(1) NQR spectra for the $4\nu_Q$ transition in $CeCoIn_5$ and Cd 1.5% doped $CeCoIn_5$ at 5 K. The frequency dependence of longitudinal nuclear spin relaxation rate $1/T_1$ is superimposed. (b) Temperature dependence of $1/T_1$ for In(1) NQR in $CeCoIn_5$ and 1.5% Cd-doped $CeCoIn_5$. The shaded area on each point reflects error associated with the measurement of $1/T_1$. The data for $CeCoIn_5$ are also plotted for a wide temperature range (from Ref. [13]). (c) Schematic illustrations for the local environment for the Cd dopants associated with 'B' and 'C' peaks in Fig. 1(a).

on the B peak. In general, $1/T_1$ is a measure of spin fluctuations, since $1/T_1$ is proportional to $T\sum_{\boldsymbol{q}} \mathrm{Im}\chi_\perp(\boldsymbol{q},\omega_0)$ where $\mathrm{Im}\chi_\perp(\boldsymbol{q},\omega_0)$ is imaginary part of dynamical spin susceptibility, $\boldsymbol{q}$ is propagation wave vector, and ω_0 is an NQR frequency. It should be noted that no enhancement of $1/T_1$ on the C peak indicates that antiferromagnetic fluctuations are not enhanced around Cd(1) dopants. The temperature dependence of $1/T_1$ for the B peak is significantly enhanced for temperatures well below T^* and less temperature dependent. Indeed, $1/T_1$ for peak B is nearly temperature independent below $\sim$10 K, as indicated by the dotted line in Fig. 1(b), although it shows a critical slowing down of $1/T_1$ just above T_N. This constant $1/T_1$ behavior indicates that the $4f$ spin fluctuations behave as if localized. On the other hand, $1/T_1$ for the bulk region in 1.5% Cd-doped $CeCoIn_5$ is nearly equivalent to that in $CeCoIn_5$. These results strongly suggest that a small group of Ce sites neighboring Cd(2) dopants remains unscreened by conduction electrons, but the majority of the Cd-doped sample is in the same electronic state as in undoped $CeCoIn_5$. Such local environments around Cd(1) and Cd(2) dopants are schematically illustrated in Fig. 1(c). Interestingly, the Cd(1) dopants do not induce local moments, proving anisotropic p-f hybridization paths between Ce-In(1) and Ce-In(2) [14], which is also experimentally suggested by the anisotropic Grüneisen parameters in $CeCoIn_5$[15].

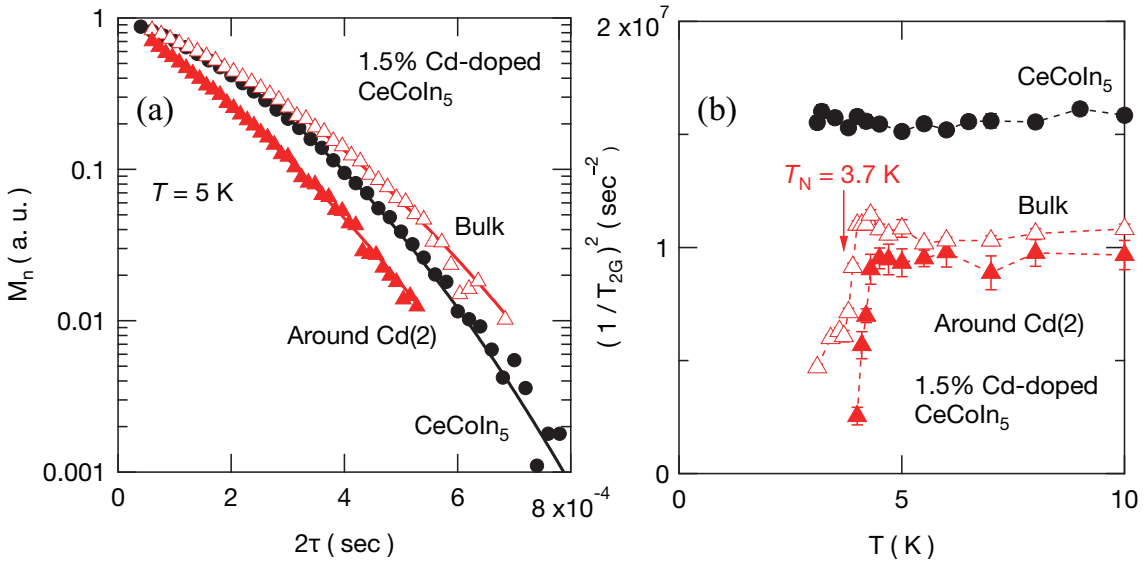

Figure 2. (a) Echo decay curves at 5 K for In(1)-NQR in $CeCoIn_5$ and 1.5% Cd-doped $CeCoIn_5$. (b) Temperature dependence of $1/T_{2G}^2$ derived from the echo decays.

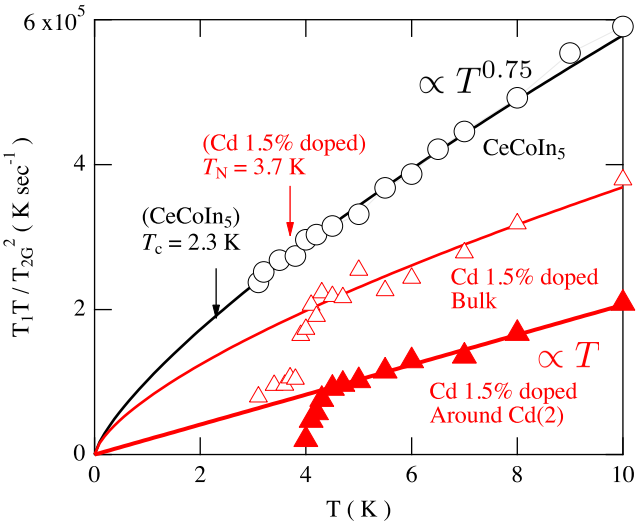

Figure 3. Temperature dependence of T_1T/T_{2G}^2 for In(1) NQR in $CeCoIn_5$ and 1.5% Cd-doped $CeCoIn_5$. The solid curves represent fits to cT^n.

For further confirmation of the local moments around Cd(2) dopants, we have measured the transverse nuclear spin relaxation rates $1/T_2$, which provide a measure of the magnetic correlation length ξ. As shown in Fig. 2(a), the obtained echo decay curves on a semi-log scale are convex upward, indicating finite Gaussian components. Since the T-dependence and orders of magnitude of the obtained $1/T_{2L}$ are consistent with $1/T_1$ values from NQR [8], our estimates of $1/T_{2G}$ are reasonable. As shown in Fig. 2(b), $1/T_{2G}^2 \propto \int \mathrm{Re}\chi^2(\boldsymbol{q},0)d\boldsymbol{q}$ [16, 17] is nearly T-independent below ∼10 K except for a decrease just above T_N in Cd-doped $CeCoIn_5$. In the paramagnetic state for a strongly correlated system, the static scaling law $\mathrm{Re}\chi(q,0) \sim \xi^2 g(q\xi,0)$ holds with a scaling function g such that $(1/T_{2G}^2) \sim \xi(T)$ [18]. $\xi(T \to 0)/a$ for pure $CeCoIn_5$ has been already estimated to be about two at the low temperature [19, 2]. The bulk T-independent values in Cd-doped crystals are reduced roughly by a factor of 1/2 to 2/3 relative to pure $CeCoIn_5$. Therefore, we deduce that Cd doping reduces ξ/a to approximately unity.

Recently, the quantity of T_1T/T_{2G}^2 has been proposed to be a measure for identifying the quantum criticality class for heavy fermion materials [20, 21]. The technical validity of this method has been originally discussed in high-T_c cuprates [22, 23]. The T-dependences of T_1T/T_{2G}^2 are discussed in Ref. [20]: it becomes (i) constant for 3D spin density wave (SDW) criticality, (ii) proportional to T in the case of localized moments, and (iii) proportional to T^α ($0 < \alpha < 1$) for 2D quantum criticality. Indeed, as shown in Fig. 3, T_1T/T_{2G}^2 for undoped $CeCoIn_5$ is found to be proportional to $T^{0.75\pm0.02}$, which is consistent with quasi-2D quantum criticality in this material. Similarly, T_1T/T_{2G}^2 for the bulk electronic state in 1.5% Cd-doped $CeCoIn_5$ shows a $T^{0.7\pm0.05}$-dependence in the temperature range $\sim 4 < T < 10$ K, although a deviation just above T_N is seen due to a critical slowing down. On the other hand, T_1T/T_{2G}^2 for the electronic state around Cd(2) dopants is proportional to T for $4.5 < T < 10$ K, again indicating the surrounding spin dynamics are dominated by localized $4f$ electrons.

4. Summary

Since NQR measurements are a powerful microscopic tool, the site-to-site relaxation rates reveal the heterogeneous electronic state in 1.5% Cd-doped $CeCoIn_5$: the majority of which is an undisturbed quantum critical metal, but the minority is localized $4f$ states confined around Cd(2) dopants. Further NQR investigations about the heterogeneous electronic states under pressures are ongoing.

5. Acknowledgments

Work at Los Alamos National Laboratory was performed under the auspices of the US Department of Energy, Office of Basic Energy Sciences, Division of Materials Sciences and Engineering. Work in Japan was partly supported by the Reimei Research Program of JAEA. section.

References

[1] Petrovic C, Pagliuso P G, Hundley M F, Movshovich R, Sarrao J L, Thompson J D, Fisk Z and Monthoux P 2001 *J. Phys. :Condens. Matter* **13** L337
[2] Sakai H, Brown S E, Baek S H, Ronning F, Bauer E D and Thompson J D 2011 *Phys. Rev. Lett.* **107** 137001
[3] Pham L D, Park T, Maquilon S, Thompson J D and Fisk Z 2006 *Phys. Rev. Lett.* **97** 056404
[4] Nicklas M, Stockert O, Park T, Habicht K, Kiefer K, Pham L D, Thompson J D, Fisk Z and Steglich F 2007 *Phys. Rev. B* **76** 052401
[5] Urbano R R, Young B L, Curro N J, Thompson J D, Pham L D and Fisk Z 2007 *Phys. Rev. Lett.* **99** 146402
[6] Seo S, Lu X, Zhu J X, Urbano R R, Curro N, Bauer E D, Sidorov V A, Pham L D, Park T, Fisk Z and Thompson J D 2014 *Nature Physics* **10** 120
[7] Sidorov V A, Nicklas M, Pagliuso P G, Sarrao J L, Bang Y, Balatsky A V and Thompson J D 2002 *Phys. Rev. Lett.* **89** 157004
[8] Sakai H, Ronning F, Zhu J X, Wakeham N, Yasuoka H, Tokunaga Y, Kambe S, Bauer E D and Thompson J D 2015 *Phys. Rev. B* **92** 121105(R)
[9] Tokiwa Y, Movshovich R, Ronning F, Bauer E D, Papin P, Bianchi A D, Rauscher J F, Kauzlarich S M and Fisk Z 2008 *Phys. Rev. Lett.* **101** 037001
[10] Booth C H, Bauer E D, Bianchi A D, Ronning F, Thompson J D, Sarrao J L, Cho J Y, Chan J Y, Capan C and Fisk Z 2009 *Phys. Rev. B* **79** 144519
[11] Kohori Y, Yamato Y, Iwamoto Y, Kohara T, Bauer E D, Maple M B and Sarrao J L 2001 *Phys. Rev. B* **64** 134526
[12] Chepin J and J H Ross J 1991 *J. Phys. :Condens. Matter* **3** 8103
[13] Yashima M, Kawasaki S, Kawasaki Y, q Zheng G, Kitaoka Y, Shishido H, Settai R, Haga Y and Ōnuki Y 2004 *J. Phys. Soc. Jpn.* **73** 2073
[14] Haule K, Yee C H and Kim K 2010 *Phys. Rev. B* **81** 195107
[15] Oeschler N, Gegenwart P, Lang M, Movshovich R, Sarrao J L, Thompson J D and Steglich F 2003 *Phys. Rev. Lett.* **91** 076402
[16] Pennington C H and Slichter C P 1991 *Phys. Rev. Lett.* **66** 381
[17] Walstedt R E and Cheong S W 1995 *Phys. Rev. B* **51** 3163

[18] Kambe S, Sakai H, Tokunaga Y, Matsuda T D, Haga Y, Chudo H and Walstedt R E 2009 *Phys. Rev. Lett.* **102** 037208
[19] Stock C, Broholm C, Hudis J, Kang H J and Petrovic C 2008 *Phys. Rev. Lett.* **100** 087001
[20] Kambe S, Sakai H, Tokunaga Y, Matsuda T D, Haga Y, Yasuoka H, Chudo H and Walstedt R E 2010 *J. Phys.: Conf. Ser.* **200** 012076
[21] Kambe S, Sakai H, Tokunaga Y, Chudo H and Walstedt R E 2010 *physica status solidi (b)* **247** 520
[22] Itoh Y, Yasuoka H, Fujiwara Y, Ueda Y, Machi T, Tomeno I, Tai K, Koshizuka N and Tanaka S 1992 *J. Phys. Soc. Jpn.* **61** 1287
[23] Curro N J, Imai T, Slichter C P and Dabrowski B 1997 *Phys. Rev. B* **56** 877